



## Design, synthesis, anti-acetylcholinesterase evaluation and molecular modelling studies of novel coumarin-chalcone hybrids

Aso Hameed Hasan, Sonam Shakya, Faiq H.S. Hussain, Sankaranarayanan Murugesan, Subhash Chander, Mohammad Rizki Fadhil Pratama, Shajarahtunnur Jamil, Basundhara Das, Subhrajit Biswas & Joazaizulfazli Jamalis

To cite this article: Aso Hameed Hasan, Sonam Shakya, Faiq H.S. Hussain, Sankaranarayanan Murugesan, Subhash Chander, Mohammad Rizki Fadhil Pratama, Shajarahtunnur Jamil, Basundhara Das, Subhrajit Biswas & Joazaizulfazli Jamalis (2023): Design, synthesis, anti-acetylcholinesterase evaluation and molecular modelling studies of novel coumarin-chalcone hybrids, Journal of Biomolecular Structure and Dynamics, DOI: [10.1080/07391102.2022.2162583](https://doi.org/10.1080/07391102.2022.2162583)

To link to this article: <https://doi.org/10.1080/07391102.2022.2162583>



View supplementary material [↗](#)



Published online: 02 Jan 2023.



Submit your article to this journal [↗](#)



Article views: 47








View related articles [↗](#)



View Crossmark data [↗](#)



## Design, synthesis, anti-acetylcholinesterase evaluation and molecular modelling studies of novel coumarin-chalcone hybrids

Aso Hameed Hasan<sup>a,b</sup> , Sonam Shakya<sup>c</sup> , Faiq H.S. Hussain<sup>d</sup>, Sankaranarayanan Murugesan<sup>e</sup> , Subhash Chander<sup>f</sup>, Mohammad Rizki Fadhil Pratama<sup>g,h</sup> , Shajarahtunnur Jamil<sup>a</sup>, Basundhara Das<sup>i</sup>, Subhrajit Biswas<sup>i</sup> and Joazaizulfazli Jamal<sup>a</sup> 

<sup>a</sup>Department of Chemistry, Faculty of Science, Universiti Teknologi Malaysia, Johor Bahru, Johor, Malaysia; <sup>b</sup>Department of Chemistry, College of Science, University of Garmian, Kalar, Kurdistan Region-Iraq, Iraq; <sup>c</sup>Department of Chemistry, Faculty of Science, Aligarh Muslim University, Aligarh, Uttar Pradesh, India; <sup>d</sup>Department of Medical Analysis, Faculty of Applied Science, Tishk International University, Erbil, Kurdistan Region-Iraq, Iraq; <sup>e</sup>Medicinal Chemistry Research Laboratory, Birla Institute of Technology & Science Pilani (BITS Pilani), Pilani, Rajasthan, India; <sup>f</sup>Amity Institute of Phytochemistry and Phytomedicine, Amity University Uttar Pradesh, Noida, Uttar Pradesh, India; <sup>g</sup>Doctoral Program of Pharmaceutical Sciences, Universitas Airlangga, Surabaya, East Java, Indonesia; <sup>h</sup>Department of Pharmacy, Universitas Muhammadiyah Palangkaraya, Palangka Raya, Central Kalimantan, Indonesia; <sup>i</sup>Amity Institute of Molecular Medicine and Stem Cell Research (AIMMSCR), Translational Cancer & Stem Cell Research Laboratory, Noida, Uttar Pradesh, India

Communicated by Ramaswamy H. Sarma

### ABSTRACT

The major enzyme responsible for the hydrolytic breakdown of the neurotransmitter acetylcholine (ACh) is acetylcholinesterase (AChE). Acetylcholinesterase inhibitors (AChEIs) are the most prescribed class of medications for the treatment of Alzheimer's disease (AD) and dementia. The limitations of available therapy, like side effects, drug tolerance, and inefficacy in halting disease progression, drive the need for better, more efficacious, and safer drugs. In this study, a series of fourteen novel chalcone-coumarin derivatives (**8a-n**) were designed, synthesized and characterized by spectral techniques like FT-IR, NMR, and HR-MS. Subsequently, the synthesized compounds were tested for their ability to inhibit acetylcholinesterase (AChE) activity by Ellman's method. All tested compounds showed AChE inhibition with IC<sub>50</sub> value ranging from 0.201 ± 0.008 to 1.047 ± 0.043 μM. Hybrid **8d** having chloro substitution on ring-B of the chalcone scaffold showed relatively better potency, with IC<sub>50</sub> value of 0.201 ± 0.008 μM compared to other members of the series. The reference drug, galantamine, exhibited an IC<sub>50</sub> at 1.142 ± 0.027 μM. Computational studies revealed that designed compounds bind to the peripheral anionic site (PAS), the catalytic active site (CAS), and the mid-gorge site of AChE. Putative binding modes, ligand-enzyme interactions, and stability of the best active compound are studied using molecular docking, followed by molecular dynamics (MD) simulations. The cytotoxicity of the synthesised derivatives was determined using the MTT test at three concentrations (100 g/mL, 500 g/mL, and 1 mg/mL). None of the chemicals had a significant effect on the body at the highest dose of 1 mg/mL.

### ARTICLE HISTORY

Received 1 August 2022  
Accepted 19 December 2022

### KEYWORDS


Acetylcholinesterase;  
coumarin; chalcone;  
cytotoxicity;  
molecular modelling

### Introduction

Alzheimer's disease (AD) is the most frequent form of dementia, characterised by a decline in intellectual ability, behavioural alteration, and impairment in daily living activities (McKhann et al., 2011; NA, 2019; Sivakumar et al., 2020). It is one of the prime causes of disability and the leading cause of death among elderly people in the world (NA, 2015; Saravanan et al., 2021). Currently, around 50 million people are living with AD, and it is expected that the number of cases will reach around 152 million by 2050. Furthermore, the total cost of a patient's care and treatment will rise, imposing an additional socio-economic burden (Brown et al., 2005; Cimler et al., 2019; Patterson, 2018). Cholinergic dysfunction has been considered to play a definitive role in the aetiology of AD due to a decrease in acetylcholine (ACh) levels in certain areas of the

brain. Acetylcholinesterase enzyme (AChE) catalyses the breakdown of ACh and ultimately decreases its concentration at the binding receptors (Hasan et al., 2019; Islam et al., 2018). This deficiency of a critical neurotransmitter, acetylcholinesterase in brain leading to the loss of intellectual abilities. Hence, inhibitors targeting AChE have become the prime approach in the management of AD and associated complications (Hardy & Selkoe, 2002; Scarpini et al., 2003). Most of the approved drugs for treatment of AD such as donepezil, galantamine and tacrine are synthetic heterocyclic compounds that act by inhibiting the cholinesterase enzymes (ChEs) and consequently enhance the level of free act at the post synaptic junction (Goyal et al., 2018; Zaout et al., 2021). Many heterocyclic compounds with coumarin as their core nucleus demonstrated potential anti-AChE activity by blocking their active sites (Bolognesi et al., 2007; Hoerr & Noeldner, 2002; Nam et al., 2014; Tasso et al., 2011).

**CONTACT** Joazaizulfazli Jamal  [joazaizulfazli@utm.my](mailto:joazaizulfazli@utm.my)  Department of Chemistry, Faculty of Science, Universiti Teknologi Malaysia, 81310 Johor Bahru, Johor, Malaysia

 Supplemental data for this article can be accessed online at <https://doi.org/10.1080/07391102.2022.2162583>.

© 2023 Informa UK Limited, trading as Taylor & Francis Group

In this respect, coumarin-based scaffolds are the subject of interest for medicinal chemists owing to their extensive biological activities such as anti-microbial (Hu et al., 2018; Zhang et al., 2004), anti-oxidant (Kostova et al., 2011; Melagraki et al., 2009; Minhas et al., 2017), anti-inflammatory (Lee et al., 2011; Melagraki et al., 2009; Minhas et al., 2017), anti-fungal (Kumar et al., 2012), anti-HIV (Huang et al., 2005), anti-coagulant (Hadjipavlou-Litina et al., 2007), anti-tumor (Huang et al., 2011; Jacquot et al., 2007; Leonetti et al., 2004), anti-tubercular (Cardoso et al., 2011; Fujikawa et al., 1969), anti-viral (Hwu et al., 2008), anti-leishmanial (Ibrar et al., 2015, 2016), anti-asthmatic (Vasconcelos et al., 2009), anti-cancer (Gomha et al., 2018; Uttarkar et al., 2022), and anti-cholinesterase activity (Anand et al., 2012; Baruah et al., 2019; Fallarero et al., 2008; Saeed et al., 2015; Şahin et al., 2022; Sameem et al., 2017). On the other hand, chalcones are considered the precursors of flavonoids and they are secondary metabolites of terrestrial plants that exhibit anti-ChE activity (Katalinić et al., 2010; Uriarte-Pueyo & Calvo, 2011). Many studies reported on the potential anti-AChE activities of chalcone derivatives (Liu et al., 2014, 2017; Mathew et al., 2016; Tran et al., 2016; Wang et al., 2017; Zhang et al., 2018). Combination of pharmacophore compounds to produce and enhance a new hybrid, this approach well-known as molecular hybridization. Herein, by using molecular hybridization strategy, we report the design, synthesis, pharmacological evaluation, cytotoxicity and molecular modelling studies of a series of novel coumarin-chalcone hybrids as AChE inhibitors. The moieties of chalcone derivatives are connected with the coumarin core *via* an aliphatic linker to generate hybrids in order to target the active sites of AChE (Figure 1). The structure-activity relationships (SARs) are also studied to explore the influence of substituents on the activity profile.

## Materials and methods

### General procedure for the synthesis of Coumarin-Chalcone hybrids (8a-n)

Anhydrous potassium carbonate (0.2 g) was added to the solution of coumarin **3** (1 mmol) and derivatives (**7a-n**) (1 mmol) in acetonitrile (30 mL). The mixture was refluxed for 22 hours and then the reaction solution was poured into ice-water (25 mL).

The precipitate was immediately formed, filtered off, washed several times with cold water, and dried to give hybrids (**8a-n**).

### ADMET profile

The drug-likeness of the synthesised compounds and their absorbance, distribution, metabolism, excretion and toxicity (ADMET) properties were achieved *in silico* by utilizing several online servers including ProTox-II, pkCSM and SwissADME, in accordance to previously reported protocol study (Hasan et al., 2022).

### In vitro inhibition study on AChE

The activity of the designed hybrids to inhibit AChE was carried out applying the modified Ellman's protocol (Elkolly et al., 2022; Ellman et al., 1961; Yang et al., 2012). Detailed procedure is described in [supplementary materials](#).

### Cytotoxicity studies

The *in vitro* cytotoxic activity of newly synthesized hybrids against normal human liver cells was evaluated by MTT assay at the three concentration (0.25 mg/ml, 0.5 mg/ml and 1 mg/ml) as per reported protocol (Hasan et al., 2022), briefly described in [supplementary materials](#).

### Molecular docking study

Molecular docking simulations of the target compounds were investigated by using the AutoDock Vina programme (Trott & Olson, 2010). The 3D crystallographic structure of the protein with reference drug (Cheung et al., 2012) (PDB code: 4EY7) was retrieved from the RSCB PDB (<https://www.rcsb.org>). This protein served as a receptor in the docking process. The file was loaded in the BIOVIA Discovery Studio Visualizer. Water molecules and co-crystallized ligand were eliminated from receptor, and the receptor was saved in the pdb format. Using AutoDock Tools (Morris et al., 1998), polar hydrogen has been added to make this receptor prepared for docking. Kollman charges of proteins have also been determined. Partial charges of the molecule were calculated using the Geistenger method.

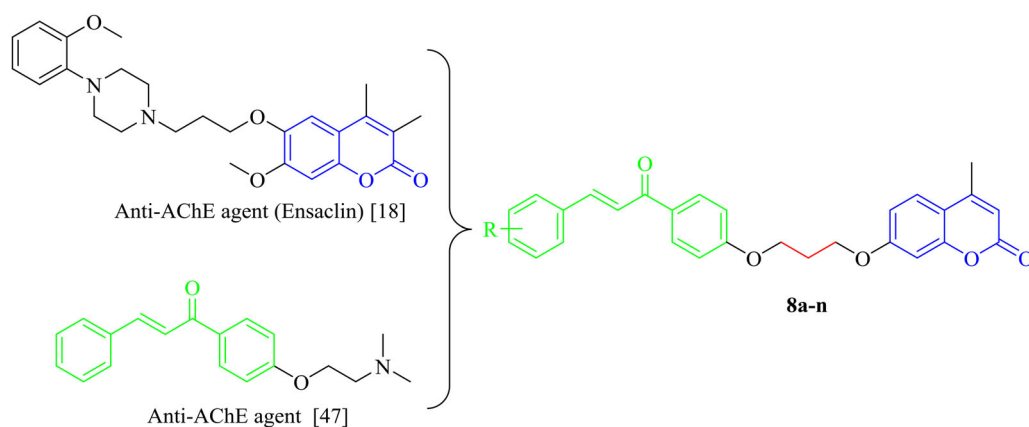


Figure 1. Design strategy for synthesis of chalcone-coumarin hybrids (8a-n).

Subsequently, the file was saved in the pdbqt format (Kawsar et al., 2021). The Avogadro programme (Hanwell et al., 2012) was utilized for drawing the structures of designed hybrids. The energy of the ligands was minimised and stored in the pdb format. The pdb file was loaded utilizing Autodock Tools. After that, it was saved in the pdbqt format. Validation was carried out by redocking the native ligand on the target protein (Nafie et al., 2019), where the native ligand was first separated from the receptor using the BIOVIA Discovery Studio Visualizer. So, docking of the test compound with the target protein can be done in the same area of the grid box where the grid box is.

The docking was performed using Autodock Vina (AV). Ligands and receptors that had been saved in the pdbqt format were copied into the Vina folder. Then, the Vina configuration file was typed into notepad. The grid box parameters values for the receptor were adjusted as center\_x = -14.108464, center\_y = -43.832714, center\_z = 27.669929, while size\_x = 40, size\_y = 40, and size\_z = 40, respectively. The default exhaustiveness value = 8 was adjusted in docking to maximise the binding conformational analysis. After that, this file is saved with the name "conf.txt." The Vina programme was run through the command prompt. The results of the docking calculation were shown in the output in notepad format. The ligands' docking conformation was determined by selecting the affinity scores (in kcal/mol) for all compounds, which were obtained and ranked based on the free energy binding theory (more negative value means greater binding affinity). The resulting structures (2D/3D) and the binding docking poses were graphically inspected to check the interactions using Discovery Studio (Accelrys Inc., San Diego, CA, USA) and Chimera software (Pettersen et al., 2004).

### Molecular dynamics (MD) simulation

The conformational space and inhibitory potential of the protein-ligand complex were studied using molecular dynamics (MD) modelling. The GROMOS96 43a1 force field, version 2019.2 of the GROMACS (GROningen MAchine for Chemical Simulations) package, was utilized to carry out molecular dynamics simulations. The latest CGenFF using CHARMM-GUI was used to produce ligand topology and parameter files (Vanommeslaeghe et al., 2010; Yu et al., 2012). To solve protein-ligand structures in a triclinic box, the SPC water model extended 10 from the protein was used (Jorgensen et al., 1983). For neutralising the systems, Na<sup>+</sup> and Cl<sup>-</sup> ions (0.15 M salt) were utilized. To remove unfavourable contact inside the system, energy minimization utilising the steepest descent method with 50,000 steps was applied. The equilibration of this complex system was obtained by following two steps. In the first step, a NVT (constant number of particles (N), constant-volume (V) and constant-temperature (T)) ensemble having constant number of particles, temperature and volume was maintained for 2 ns, this ensemble is referred to as "isothermal-isochoric." In the second step, a NPT (NVT (constant number of particles (N), constant pressure (P) and constant-temperature (T)) ensemble containing a constant number of particles, temperature and pressure was equilibrated for 10 ns. In the NPT/NVT equilibration run, the system was subjected to periodic boundary conditions at constant temperature (300 K) and pressure (1.0 bar) for 100 ns using a

Leap-frog MD integrator (Allen & Tildesley, 2017). Non-bonded interactions were truncated across 10 and 12 Å using the force-based switching method, and for electrostatic interactions, the particle-mesh Ewald technique was applied to interactions (Essmann et al., 1995). To remove unfavourable contact inside the system, energy minimization utilising the steepest descent method with five thousand steps was applied. Adding to this, the indexing system used temperature coupling between the water and non-water parts to avoid the hot solvent-cold solute problem. GROMACS analysis techniques were used to do trajectory analysis. We calculated the root mean square deviation (RMSD) and root mean square fluctuation (RMSF) of proteins using the gmx rms and gmx rmsf programmes, respectively. The gmxsasa and gmx gyrate tools were used to calculate solvent accessible surface area and the radius of gyration, respectively. Hydrogen bonds were analysed using the gmxhbond programme. Grace Software was used to create the plots, while PyMol and VMD were utilised to visualise the complicated structure (DeLano & Bromberg, 2004; Humphrey et al., 1996). The simulations were conducted on a 64-bit Intel (R) Xeon (R) CPU E5-2680 v4 running at a clock speed of 2.40 GHz. The protein-ligand complex simulation took 36.3 hours for 100 ns. MD simulations taking orders of magnitude longer to complete than computational docking.

## Results and discussion

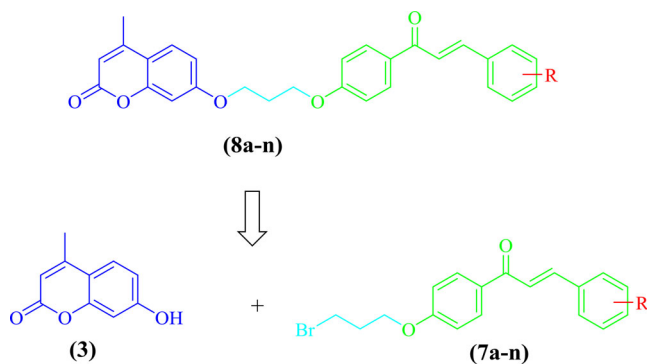
### Rational design of target hybrids

Coumarins containing compounds have been frequently reported in the areas of organic and medicinal chemistry. Moreover, 4 and 7 substituted coumarins and derivatives of chalcones have been reported as potential scaffolds for AChE inhibition activity (Kontogiorgis et al., 2012). Consequently, based on the aforesaid literature reports and taking into account the structural aspects of these pharmacophores, we envisioned generating the hybrids originating from the incorporation of the coumarin into the chalcone scaffold as anti-acetylcholinesterase agents. In the current study, 7-hydroxy-4-methylcoumarin **3** was selected as the parent pharmacophore to design titled hybrids (**8a-n**). After that, molecular docking simulation as a predictive tool was employed on the designed hybrids to identify their potencies based on binding affinities (Khodair et al., 2019; Marzouk et al., 2020). The retrosynthetic analysis was used to find suitable reactions and reagents to synthesize the target hybrids. The retrosynthetic approach was carried out in order to synthesise coumarin-chalcones (**8a-n**). Scheme 1 shows the retrosynthetic analysis of hybrids (**8a-n**). The Pechmann condensation of resorcinol **1** with ethyl acetoacetate **2** was carried out to form 7-hydroxy-4-methylcoumarin **3**. In the meantime, the Claisen-Schmidt condensation of 4-hydroxyacetophenone **4** and various benzaldehyde derivatives under basic conditions in ethanol gave chalcones (**5a-n**) were carried out. The alkylation reaction of compounds (**5a-n**) by 1,3-dibromopropane **6** afforded intermediates (**7a-n**). Finally, coumarin hybrids (**8a-n**) were synthesised from the compounds (**7a-n**) and **3**.

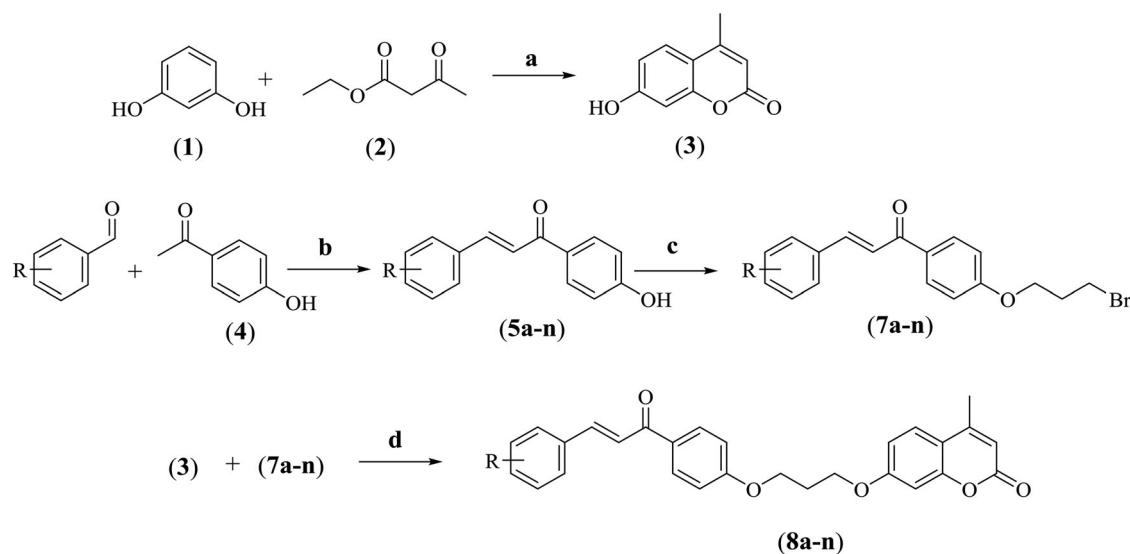
### Synthetic routes

The synthetic route of target compounds (**8a-n**) is outlined in Scheme 2. The Pechmann condensation of resorcinol **1** with ethyl acetoacetate **2** in dioxane in the presence of a catalytic amount of concentrated sulphuric acid under reflux for 4 hours, gave 7-hydroxy-4-methylcoumarin **3** in a good yield. On the other hand, treatment of 4-hydroxyacetophenone **4** with various benzaldehydes in absolute ethanol *via* base catalysed Claisen-Schmidt condensation, stirred for 24 hours at room temperature, produced chalcones (**5a-n**). The obtained chalcones (**5a-n**) were then reacted with an excess of dibromopropane **6** in the presence of anhydrous  $K_2CO_3$  in boiled  $CH_3CN$ , stirred for 7 hours, affording the key intermediates (**7a-n**), which were finally reacted with the corresponding coumarin **3** to obtain the desired hybrids (**8a-n**).

The structures of hybrids (**8a-n**) were elucidated by IR,  $^1H$  NMR, and  $^{13}C$  NMR. The IR spectra of exhibited absorption bands of  $C=C$  (aromatic and olefinic),  $C=O$  (ketone and lactone),  $C-H$   $sp^3$ ,  $C-H$   $sp^2$ . A strong absorption bands of  $C=O$  (ketone) could be found in  $1654-1660\text{ cm}^{-1}$ , whereas  $C=O$  (lactone) bands were observed around  $1724-1736\text{ cm}^{-1}$ . The  $^1H$  NMR spectra of hybrids (**8a-n**) demonstrated that the reaction was complete when the triplet signal in the range of  $3.63-3.60$  disappeared, corresponding to the  $(-CH_2Br)$  group



Scheme 1. Design of hybrids (**8a-n**) as potential anti-AChE agent



Scheme 2. Synthesis of chalcone-coumarin hybrids (**5a-n**). Reagents and conditions: (a) dioxane,  $H_2SO_4$ , reflux, 4 h; (b) NaOH, absolute ethanol, rt, 24 h; (c) dibromopropane, anhydrous  $K_2CO_3$ ,  $CH_3CN$ , reflux, 7 h; (d) anhydrous  $K_2CO_3$ ,  $CH_3CN$ , reflux, 22 h.

being replaced by the  $(-CH_2O)$  group. Each hybrid's spectrum revealed signals for the leftover protons in a manner almost identical to that of its starting materials. The structures of coumarin-chalcones (**8a-n**) were further validated using  $^{13}C$  NMR analysis, which revealed two peaks corresponding to carbonyl groups in the downfield region. The  $C=O$  groups of the chalcone moiety were determined to be between 187.7 and 188.8, whereas those of coumarin were determined to be between 161.7 and 161.8. Additionally, the spectra revealed signals for the *trans*-olefinic carbons of the chalcone core in hybrids (**8a-n**) at 199.5–125.6 ( $C-\alpha$ ) and 139.8–144.1 ( $C-\beta$ ) (Banerjee et al., 2018; Kalepu & Nekkanti, 2015; Luscombe et al., 2001; Picciotto et al., 2012; Savjani et al., 2012; Vilar et al., 2010; Wade & Goodford, 1989). The remaining carbon atoms were found in the aromatic area as expected.

### In silico drug-likeness and ADMET profiles

The drug-likeness and ADMET profiles of all hybrids were calculated *in silico* as presented in Table 1. The obtained findings were compared to the optimum range (Table S1) and Lipinski's rule of five was referenced (LRO5) (Hasan et al., 2022; Prasanna & Doerksen, 2009; Salih et al., 2022). The first parameter examined was Mol Wt, in which three derivatives (**8a-g**) did not meet the LRO5 criteria ( $\leq 500$  g/mol). However, all three still met the criteria set by Chander et al. (Chander et al., 2016). Only compounds **8h** and **8i** met the criteria for TPSA values, the rest showed TPSA values less than  $90\text{ \AA}^2$ . However, these two compounds did not meet the optimum criteria for the amount of HBD ( $> 7$ ), while all compounds did not meet the criteria for the amount of HBA (0). All compounds had relatively large log P values and did not meet the LRO5 criteria ( $> 5$ ) (Prasanna & Doerksen, 2009). However, only three compounds (**8a-g**) were outside the optimal range. Consistent with their log P values, the log S of all compounds also did not meet the criteria, indicating poor water solubility. Even so, the  $Caco_2$  value of all compounds was still within optimal limits criteria (Chander et al., 2016; Salih et al., 2022). All compounds

showed log BB values lower than  $-0.3$ , in which compounds **8h** and **8i** were even lower than  $-1.1$ . The low log BB value indicates that these compounds may have poor distribution to the brain and may not be suitable to target the brain and CNS (Vilar et al., 2010). However, since the target receptor in this study is AChE which is not only found in the brain but also in other parts of the body (Picciotto et al., 2012), these compounds may inhibit AChE in organs aside brain and contribute to Alzheimer's therapy.

Meanwhile, the number of rotatable bonds of all compounds (9–10 bonds) are in the optimal range. From the properties of ADME, there are at least two challenges that can be faced in developing these compounds as drugs. First is the presence of hydrogen bond groups, both as donors and acceptors. The relatively large number of hydrogen donors not accompanied by hydrogen acceptors will limit the choice of ideal binding sites for target receptors (Wade & Goodford, 1989), especially those with many amino acids with hydrogen donor atoms such as arginine (Luscombe et al., 2001). The replacement of some substituents that are hydrogen donors into hydrogen acceptor groups can be a rational strategy to overcome these challenges. Second, is low water solubility and high lipophilicity. Challenges will be faced even before the drug enters the body, starting with the formulation process. As it is known, water is the most commonly used solvent in the formulation process of drug preparations (Savjani et al., 2012). Therefore, low water solubility can prolong the manufacturing process of drug preparation, complicate the manufacturing process, and ultimately increase the cost of production (Kalepu & Nekkanti, 2015). Accordingly, the selection of oral dosage forms may be more challenging, and consideration should be given to other dosage forms suitable for the nature of the compounds. ProTox-II was used to examine the toxicity of each compound, as shown in Figure S1. The toxicity of all compounds is relatively mild to moderate, with pLD<sub>50</sub> values ranging from 950 to 3000 mg/kg, or class IV-V in the globally harmonised system of classification of chemicals (Banerjee et al., 2018), and none of them showed a positive Ames test result from pkCSM. However, the results with ProTox-II for compounds **8h** and **8i** showed a high probability ( $> 0.7$ ) of

mutagenicity (mutagen). Carcinogenicity (carcino), immunotoxicity (immuno), and stress response pathways to mitochondrial membrane potential (sr mmp) were some of the additional toxicity targets observed. However, only immuno and mutagen properties show a high probability. Compounds **8h** and **8i** also had the most toxicity targets with three targets, followed by compounds **8a**, **8e**, **8f**, and **8j** with two targets, and the rest each had the same target: immuno. It should be noted that compounds **8a**, **8e**, **8f**, and **8j** have a probability of being carcinogens, although with a low probability (0.7). Overall, compounds (**8e-i**) show flaws in the properties of ADME, while compounds **8h** and **8i** also tend to be more toxic, although compound **8i** shows the highest pLD<sub>50</sub> value. Thus, other compounds such as **8b**, **8c**, **8d**, **8k**, **8l**, **8m**, and **8n** have more ideal ADMET properties to be developed as drug compounds than other test compounds.

### Anti-acetylcholinesterase Coumarin-Chalcone hybrids (8a-n)

The inhibitory activity of the target hybrids coumarin-chalcones (**8a-n**) and the standard drug galantamine against AChE was determined. The investigation discovered that all hybrids exhibited a high level of inhibitory activity. Anti-AChE screening was performed by altering the aromatic substitutions at the imine and chalcone backbones. The anti-AChE potency was investigated using various electron-withdrawing groups (Br, Cl, and NO<sub>2</sub>) and electron-donating groups (CH<sub>3</sub> and OCH<sub>3</sub>) on the aromatic rings of the chalcone side, as well as without substituents. Two aspects influence the anti-AChE activity of these hybrids: the nature and position of the substituents. The biological screening data for these derivatives enables us to postulate the synthesised compounds' structure-activity relationship (SAR).

All target molecules (**8a-n**) were tested for AChE inhibitory activity. The results were compared to the reference drug in terms of IC<sub>50</sub> values. Based on the data presented in Table 2, the structure activity relationship (SAR) demonstrated potent AChE inhibitory action with IC<sub>50</sub> values ranging from 0.201 to 1.047  $\mu$ M, which was less than the standard drug, galantamine, at 1.142  $\mu$ M. Without a substituent, compound **8a** exhibited

**Table 1.** *In-silico* predicted physicochemical and ADMET parameters.

Compounds	Mol Wt <sup>a</sup>	TPSA <sup>b</sup>	HBD	HBA	log P	log S <sup>c</sup>	Caco2 <sup>d</sup>	log BB	Rot	Acute tox. <sup>e</sup>	pLD <sub>50</sub> <sup>f</sup>	Ames
8a	440.495	65.74	5	0	5.84542	-7.212	0.472	-0.4	9	IV	1500	No
8b	474.94	65.74	5	0	6.49882	-7.376	0.492	-0.428	9	IV	950	No
8c	474.94	65.74	5	0	6.49882	-7.382	0.481	-0.444	9	IV	950	No
8d	474.94	65.74	5	0	6.49882	-7.381	0.486	-0.448	9	IV	1500	No
8e	519.391	65.74	5	0	6.60792	-7.405	0.483	-0.429	9	IV	1500	No
8f	519.391	65.74	5	0	6.60792	-7.411	0.472	-0.445	9	IV	1500	No
8g	519.391	65.74	5	0	6.60792	-7.411	0.478	-0.449	9	IV	1500	No
8h	485.492	111.56	7	0	5.75362	-6.802	0.583	-1.11	10	IV	1500	No
8i	485.492	111.56	7	0	5.75362	-6.79	0.579	-1.106	10	V	3000	No
8j	470.521	74.97	6	0	5.85402	-6.794	0.985	-0.829	10	IV	1500	No
8k	470.521	74.97	6	0	5.85402	-7.161	0.536	-0.829	10	V	2500	No
8l	454.522	65.74	5	0	6.15384	-7.289	0.541	-0.414	9	IV	1500	No
8m	454.522	65.74	5	0	6.15384	-7.295	0.53	-0.431	9	V	2652	No
8n	454.522	65.74	5	0	6.15384	-7.29	0.536	-0.435	9	IV	1500	No

<sup>a</sup>Molecular weight in g/mol.

<sup>b</sup>Topological polar surface area in Å<sup>2</sup>.

<sup>c</sup>Aqueous solubility in log mol/L.

<sup>d</sup>Predicted apparent Caco-2 cell permeability in 10<sup>-6</sup> cm/s.

<sup>e</sup>Acute toxicity according to the globally harmonized system (GHS) of classification and labelling of Chemicals.

<sup>f</sup>Predicted LD<sub>50</sub> in mg/kg.

good activity against the enzyme, with an  $IC_{50}$  value of  $0.457 \mu\text{M}$ . Electron-withdrawing groups on C-2 or C-4 of ring-B compounds (except for compound **8h**) seem to make them more effective against AChE than **8a**. This may be attributed to local electron-deficient sites in the aromatic molecule that interact strongly with the amino acids present in the enzyme (Nepali et al., 2019). The order of decreasing inhibition of these hybrids (**8b-i**) against AChE can be arranged as follows: 2-Cl (**8d**) > 2-Br (**8g**) > 4-Cl (**8b**) > 4-Br (**8e**) > 4-NO<sub>2</sub> (**8h**). On the other hand, the electron-donating bearing compounds (**8j-n**) showed diminished activity toward the enzyme compared to parent hybrid **8a**, which had no substituent. As shown in the table, these hybrids having substituent at the C-3 position of the chalcone aromatic ring-B exhibited better activity than those with substituent at the C-2 or C-4 position, and the sequence was: 3-CH<sub>3</sub> (**8m**) > 3-OCH<sub>3</sub> (**8k**) > 4-OCH<sub>3</sub> (**8j**) > 2-CH<sub>3</sub> (**8n**) > 4-CH<sub>3</sub> (**8l**). The results indicate that the electron-withdrawing groups (**8c**, **8f** and **8i**) at the C-3 position decrease the inhibitory activity against AChE. It is worth mentioning that among all the hybrids (**8a-n**), **8d** was the most active with an  $IC_{50}$  value of  $0.201 \mu\text{M}$ , showed five folds higher activity compared to galantamine, while compound **8l** ( $IC_{50} = 1.142 \mu\text{M}$ ) was the least active against AChE. As shown in Figure 2, it can be concluded from the SAR analysis of the synthesised hybrids (**8a-n**) that the presence of electron withdrawing groups on the C-2 or C-4 phenyl ring-B in the chalcone moiety played an essential role in the activity. In particular, chloro or bromo on

C-2 showed significant favoured activity, as shown with compounds **8d** and **8g**.

### Cytotoxicity studies

At the tested concentration of  $0.25 \text{ mg/ml}$  (lowest tested concentration), all compounds showed % cell viability more than 85%. Moreover, except four compounds (**8b**, **8c**, **8j** and **8l**), all other shows cell viability greater 90% in comparison to the control group. Least cell viability was observed in the cell group treated with compound **8b** (85.87%). At the next higher concentration ( $0.5 \text{ mg/ml}$ ), interestingly majority of the compounds showed more than 90% cell viability, except compound **8m** which showed slightly less cell viability (88.45%). Upon further

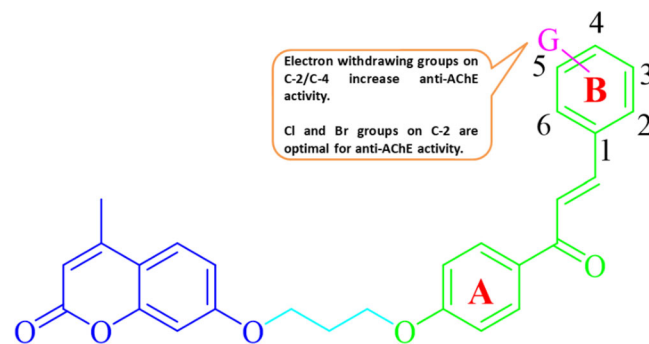


Figure 2. Structural activity relationships of the titled compounds (**8a-n**).

Table 2. The docking scores and  $IC_{50}$  values of the designed compounds (**8a-n**) and standard drug against AChE.

Co.	G	Molecular docking scores				Bioassay	
		B. E. (kcal/mol)	Polar Interactions (Hydrogen Bond)	Hydrophobic Interactions	IC (Ki)	$IC_{50}$ [ $\mu\text{M}$ ]	
<b>8a</b>	H	-12.2	HIS447, SER203, GLU202, ASN87, PRO88	TYR337, TRP286, TYR124, TRP86	396.69 pM	$0.457 \pm 0.021$	
<b>8b</b>	4-Cl	-11.9	THR75, LEU76, TYR337, TRP86	TYR341, ILE451, TYR133	818.37 pM	$0.262 \pm 0.007$	
<b>8c</b>	3-Cl	-12.1	GLY121, GLY122, SER203, PHE295	TRP86, TYR124, TRP286, LEU289, PHE338	502.05 pM	$0.648 \pm 0.030$	
<b>8d</b>	2-Cl	-12.3	TYR72, THR75	LEU76, TRP86, TRP286, VAL294, PHE338, TYR341	186.04 pM	$0.201 \pm 0.008$	
<b>8e</b>	4-Br	-11.9	SER125, TYR133, SER203, GLU202, HIS447	TRP86, TYR124, TRP286, TYR337	800.83 pM	$0.265 \pm 0.013$	
<b>8f</b>	3-Br	-11.8	GLY121, TYR124, GLU202, SER203, TYR341	TRP286, TYR337, PHE338	969.95 pM	$0.814 \pm 0.034$	
<b>8g</b>	2-Br	-12.2	TYR72, TYR124, SER293, VAL294	LEU76, TRP86, TRP286, TYR337, TYR341	397.11 pM	$0.240 \pm 0.014$	
<b>8h</b>	4-NO <sub>2</sub>	-11.6	TYR72, THR75, TYR133, TYR341	LEU76, TRP86	1.61 nM	$0.576 \pm 0.066$	
<b>8i</b>	3-NO <sub>2</sub>	-12.0	TRP86, SER293, PHE295, TYR337	TRP286, LEU289, TYR337, PHE338	817.95 pM	$0.737 \pm 0.018$	
<b>8j</b>	4-OCH <sub>3</sub>	-11.4	GLY120, PHE295, ARG296	TRP86, TRP286, PHE338, TYR341	1.84 nM	$0.907 \pm 0.023$	
<b>8k</b>	3-OCH <sub>3</sub>	-12.2	TYR72, SER293, PHE295	TRP286, TYR337, PHE338, TYR341	397.32 pM	$0.590 \pm 0.027$	
<b>8l</b>	4-CH <sub>3</sub>	-11.7	TYR72, THR75, PHE295	LEU76, TRP86, PHE297, TYR341, HIS447	1.05 nM	$1.047 \pm 0.043$	
<b>8m</b>	3-CH <sub>3</sub>	-12.3	SER293, PHE295	TRP86, TRP286, LEU289, TYR337, PHE338, TYR341	186.71 pM	$0.579 \pm 0.011$	
<b>8n</b>	2-CH <sub>3</sub>	-11.4	TYR124, GLU292, SER293, PHE295	HIS287, LEU289, TYR37, PHE338, TYR341, HIS447	1.75 nM	$0.966 \pm 0.024$	
Gal.	-	-9.6	GLN71, TYR72, TRP86, ASN87, TYR124, GLU202, PHE338	TYR341	674.25 nM	$1.142 \pm 0.027$	

Data are expressed as mean  $\pm$  Standard Deviation of seven independent experiments performed in triplicate. Co.: compound, B.E: binding energy, and Gal.: standard drug (Galantamine).

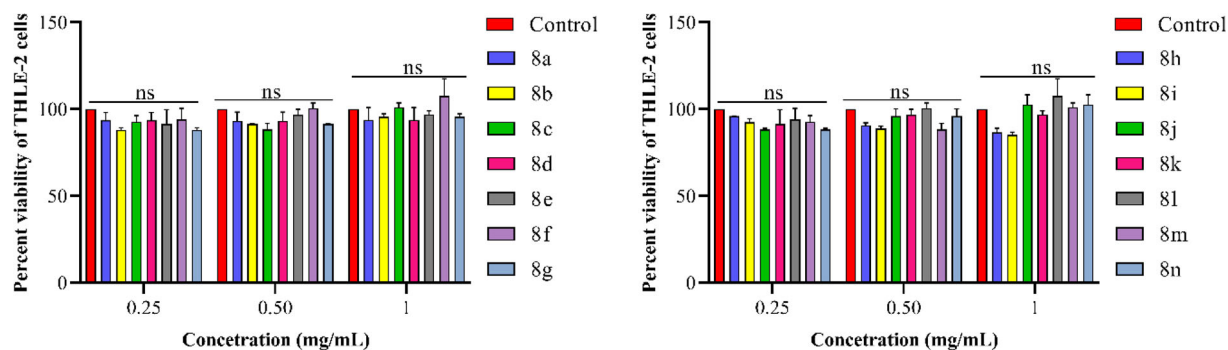


Figure 3. Cytotoxicity results of the titled compounds (**8a-g**).

increasing the concentration (1.0 mg/ml), two compounds (**8i** and **8j**) slightly decreased the cell viability (86.73 and 85.71%, respectively), while no significant effect on cell viability was observed on wells treated with other compounds.

Overall, not much significant change in cell viability was observed between the compound treated and control wells for normal human liver cells (THLE-2), even at the highest tested concentration of 1000  $\mu\text{g}/\text{mL}$  (1 mg/ml) of compounds. So, it can be concluded that the tested compounds have little to no effect on viability of normal human liver cell line and compounds can be considered non cytotoxic (Figure 3).

## Docking studies

Molecular docking simulations were used to determine the probable positions of the targeted ligands in the active site

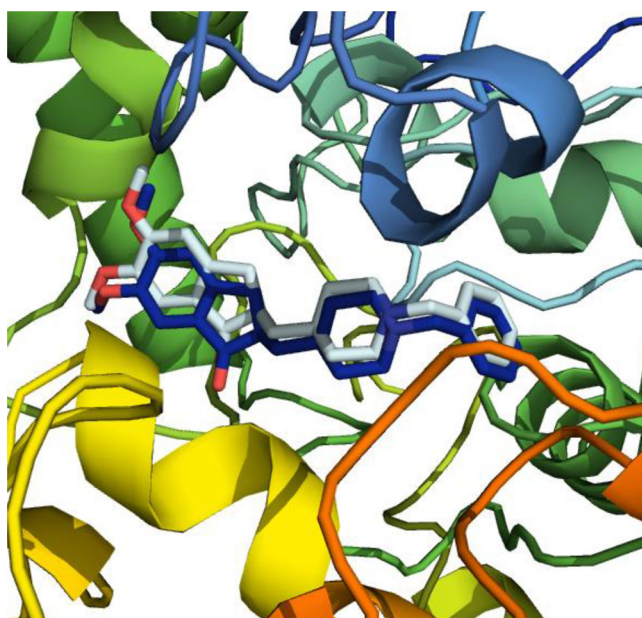


**Figure 4.** Superimposition of the re-docked donepezil (gray color) and co-crystallized ligand (blue color).

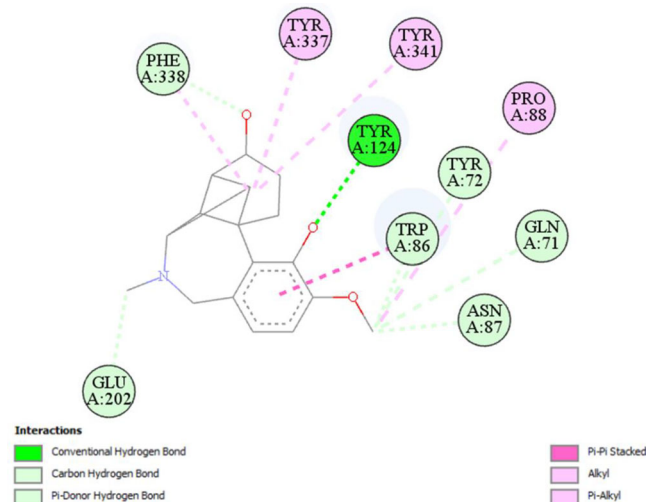


**Figure 5.** Illustration of the interactions of galantamine in the active site of AChE (PDB ID: 4EY7).

of the enzyme (AChE). Initially, to verify the docking method, the co-crystallized ligand, donepezil (E20) in the 3D x-ray crystal structure was re-docked against the active site of the enzyme (Figure 4). The re-docked pose showed the perfect

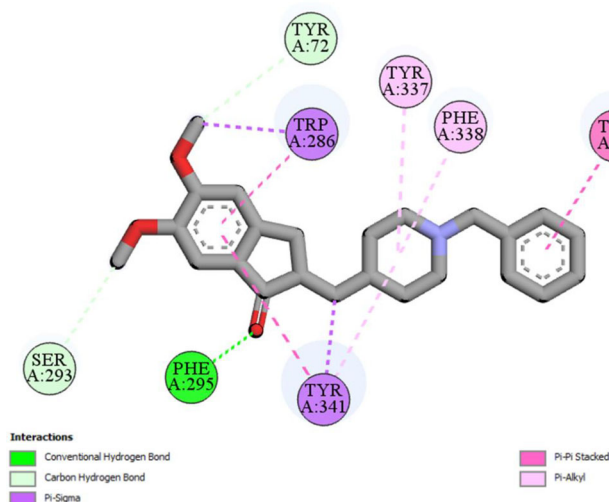


**Figure 6.** 2D representation of interactions of co-crystallized ligand in the active site of AChE (PDB ID: 4EY7).

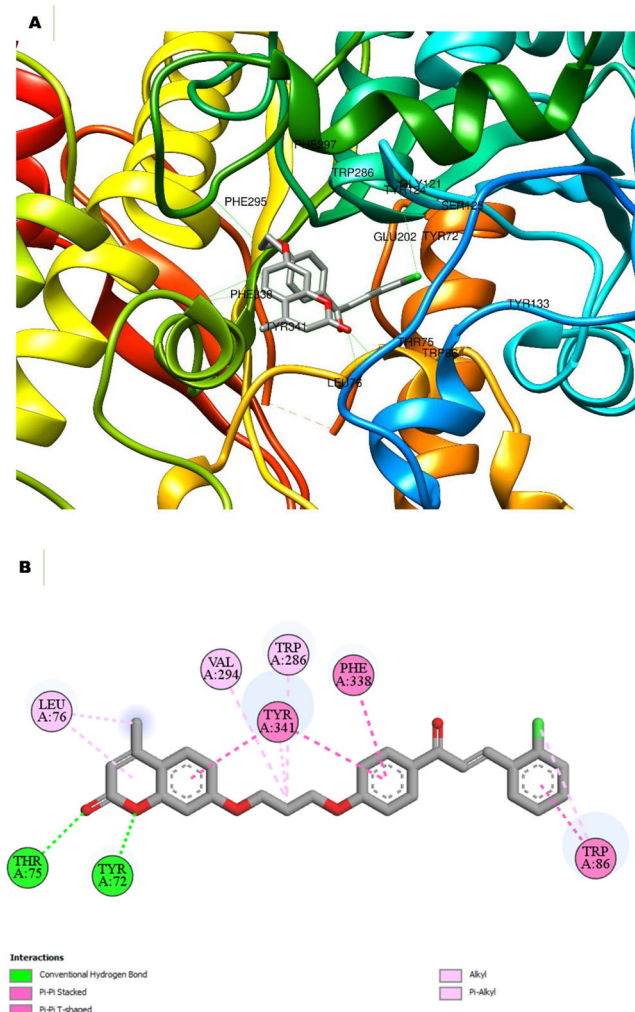


**Figure 7.** (a) 3D and (b) 2D representation of interactions of compound **8d** in the active site of AChE (PDB ID: 4EY7).



superimposition at the binding site with low RMSD value = 0.69 Å indicating validity of the docking procedure. Thus, could be considered as an active binding site (Hussen et al., 2022; Poli et al., 2016). After that, the synthesized compounds were subjected to docking to the defined binding site. As shown in Figure 5, the docked pose accomplished by positive control, galantamine involved H-bond of TYR124 residues with the oxygen atom. Two hydrophobic interactions including  $\pi$ -alkyl and  $\pi$ - $\pi$  stacked interactions were formed between rings of the galantamine and TRP86. Another  $\pi$ - $\pi$  stacked interaction was also found with TYR341. Additional five H-bonds, carbon hydrogen and  $\pi$ -hydrogen bonds were also established with amino acid residues GLN71, TYR72, ASN 87, TRP86 and PHE338.

Docking studies of the native inhibitor, donepezil occupied the PAS region on the active site of acetylcholinesterase forming  $\pi$ -sigma,  $\pi$ - $\pi$  stacked interactions with amino acid residue of PHE286 and carbon H-bond with TYR72. In contrast, it was found in the CAS region, established two hydrophobic alkyl interaction with TYR337 and PHE338 residues and one  $\pi$ - $\pi$  stacked interaction with TRP86. Additionally, donepezil oriented towards mid-gorge of the target enzyme, which was participated with SER293 (carbon hydrogen bond), PHE295 (H-bond) and TYR341 ( $\pi$ -sigma and  $\pi$ - $\pi$  stacked interactions) (Figure 6).

The binding energy value with the lowest value corresponds to the compound's optimal conformational position within the active region of the targeted protein. According to the docking results (Table 2), all of the synthesised hybrids

(-11.4 to -12.3 kcal/mol) exhibited significant and better activity against AChE when compared to the control drug galantamine (-9.6 kcal/mol). The docking investigations of the most potent hybrid **8d** with AChE indicated that this hybrid was capable of binding not only to dual sites (CAS and PAS), but also to AChE's mid-gorge site (Figure 7). The amino acids TYR72 and THR75 form two important hydrogen bonds in the PAS region, where both oxygen atoms are found in the coumarin moiety of the amino acids. In the CAS, the rings of the chalcone skeleton interacted with TRP86 and PHE338 via  $\pi$ - $\pi$ -stacked interaction. Additionally, significant interactions between aromatic rings of chalcone and coumarin moieties with TYR341 were observed in the middle gorge area. Coumarin's methyl group can form an alkyl bond with LEU76. Another alkyl interaction was observed between aliphatic linker and VAL294. Moreover, interactions (alkyl and  $\pi$ -alkyl) between the chloro atom and the coumarin core were identified for the amino acids TRP86. The amino acid residues of TRP286 could interacted with linker through  $\pi$ -alkyl interaction. The binding energy generated was -12.3 kcal/mol, which was greater than the binding energy generated by standard drug interactions (Table 2).

### Molecular dynamics simulation

A 100 ns MD simulation was performed with the best posed model having the top AutoDock Vina docking score for the protein-ligand interaction. The best docking outcome was used to set up this procedure in a high-throughput way and to

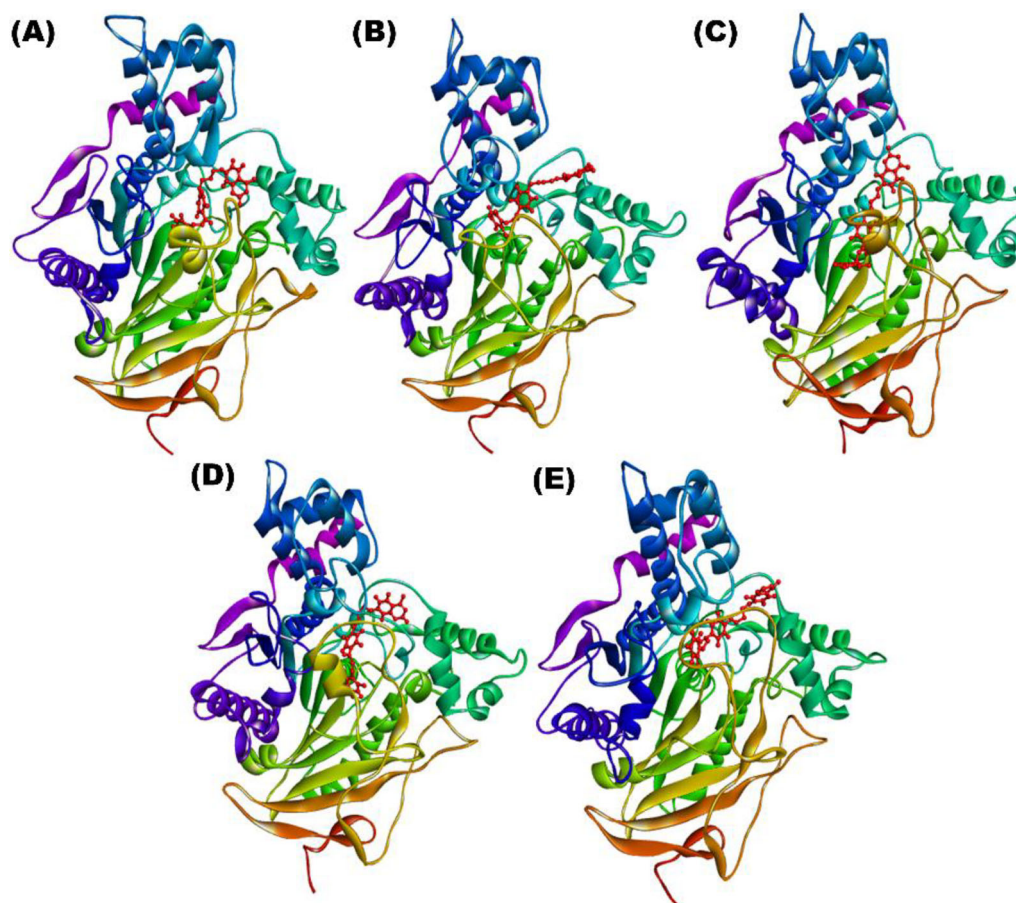
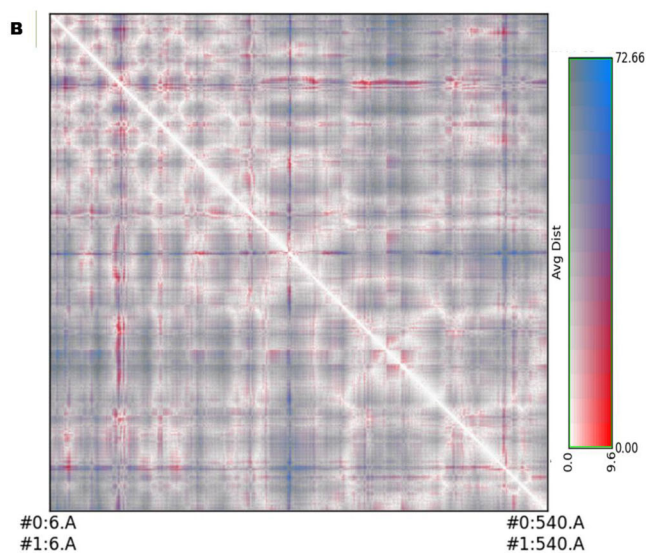
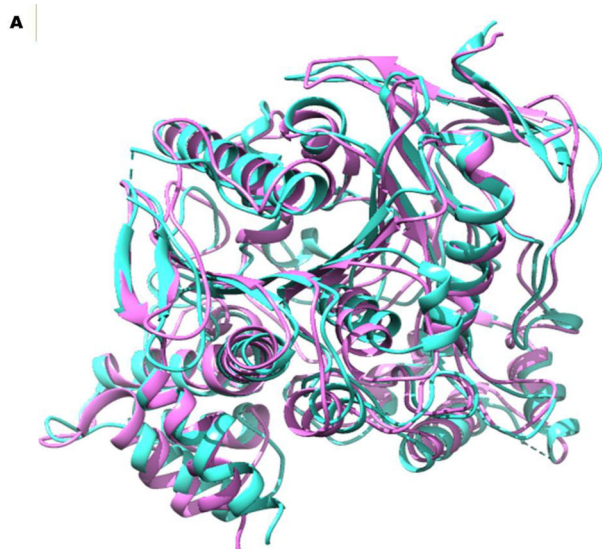
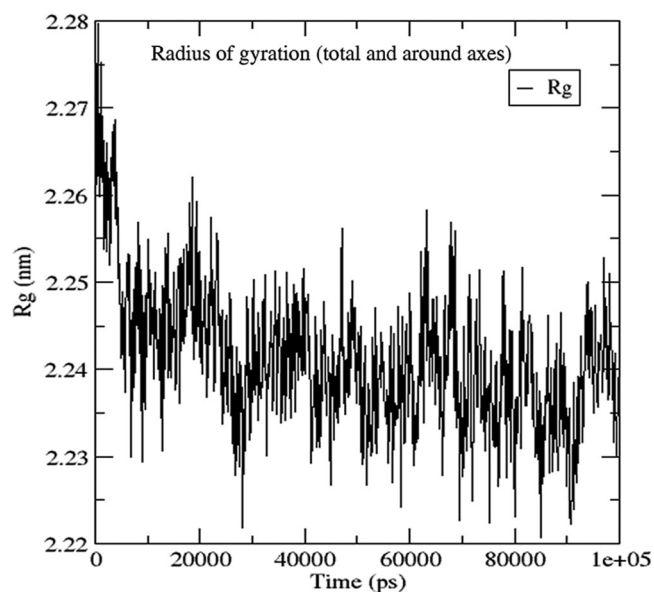


Figure 8. Protein-ligand structure at (a) 1 ns, (b) 10 ns, (c) 20 ns, (d) 50 ns and (e) 100 ns MD run where ligand is in red color.



**Figure 9.** (a) Superimposed structure of protein before MD simulation (blue) and after MD simulation (purple) and (b) RR distance map displaying patterns of spatial interactions of the target protein.

investigate the interaction mechanism dynamics of the molecule at the active site of the enzyme under stated water conditions. As shown in Figure 8, the conformational changes of the protein-ligand complex were investigated over the 1, 10, 20, 50, and 100 ns MD production runs. To analyse the structural stability, molecular dynamics information is treated by calculating the RMSD (from the initial structure). The RMSD value of the protein-ligand complex was found to be  $\sim 2.72$  Å (Figure S2). The RMSD plot demonstrates that the protein-ligand complex established a stable conformation after  $\sim 60$  ns with an acceptable RMSD value of 2.6. The range of RMSD values below 3.0 is generally acceptable, as the lower the RMSD value, the more stable the system (Kufareva & Abagyan, 2012). The RMSF enables the analysis of the average fluctuation as well as the flexibility of amino acids in the protein and demonstrates that fluctuations in amino acid residues occur numerous times during the protein's ligand-bound state (Figure S3).



**Figure 10.** Radius of gyration (Rg) of protein-ligand complex during 100 ns simulation time.

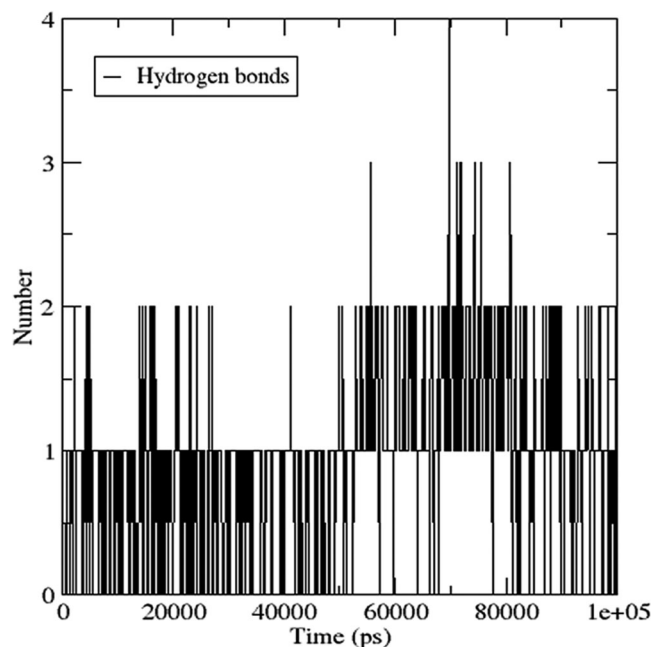


**Figure 11.** Number of average hydrogen bonding interactions between protein-ligand complex during 100 ns simulation time.

The findings suggest that ligand-protein interaction brings protein chains closer together, which reduces the distance between them, as shown in Figure 9(a). Meanwhile, in Figure 9(b), the RR distance map depicts patterns of spatial interactions (2-D representations of protein 3 D structure) residues (Hussen et al., 2022; Khan et al., 2021; Wu & Zhang, 2008). The acquired data revealed a drop in the radius of gyration (Rg) for the protein-ligand complex as the simulation time progressed, indicating an increase in the structure's compactness (Figure 10). Grid-search on a 16x16x19 grid with  $rcut = 0.35$  was used to calculate and plot the number of intermolecular hydrogen bonds between protein and ligand, as shown in Figure 11. There were 737 donors and 1472 acceptors detected when hydrogen bonds between ligand (45 atoms) and protein (5270 atoms) were

calculated. We found that 0.982 of 542432 potential hydrogen bonds were observed in each timeframe. A significant increase in the number of hydrogen bonds was found when ligands and proteins interacted. The SASA of the protein was calculated during the MD simulation in the ligand-bound state, which illustrates the change in SASA values caused by the ligand binding to the protein (Figure S4). In general, the results demonstrate the folding states of the protein and its stability when bound to a ligand.

## Conclusion

A novel series of coumarin-chalcone hybrids (**8a-n**) was designed using molecular docking research. The affinity energies of these hybrids (**8a-n**) for the active site of acetylcholinesterase (AChE) were reported to be between  $-10.6$  and  $-13.2$  kcal/mol, while the positive control, galantamine, had an affinity energy of  $-9.6$  kcal/mol. The in-silico results indicated that most of the proposed hybrids had higher inhibition activity than the positive controls. The designed hybrids have been successfully synthesised and their inhibitory activities on the AChE were evaluated using Ellman's protocol. Galantamine was employed as a positive control with an  $IC_{50}$  of  $1.142 \pm 0.027$  M. The bioassay results ( $IC_{50}$  values ranging from 0.201 to 1.047 g/mL) indicated that all these synthesised compounds had the capacity to inhibit AChE activity. Particularly, hybrids **8d** bearing Cl substituent at C-2 on the ring-B of chalcone scaffold ( $IC_{50} = 0.201 \pm 0.008$   $\mu$ M) and **8g** having Br substituent at C-2 on the ring-B of chalcone scaffold ( $IC_{50} = 0.240 \pm 0.014$   $\mu$ M) showed the most effective AChE inhibitory activity, which were about six folds better than galantamine. At the highest dose of 1000 g/mL, none of the compounds had a big effect on normal human liver cells (THLE-2). Moreover, molecular docking was used to investigate the type of interaction between the synthesised compounds (**8a-n**) and the active site of a related enzyme. The results demonstrated that most hybrids exhibit hydrogen bonding and hydrophobic interactions like  $-\sigma$ ,  $-\text{stacking}$ ,  $-\text{alkyl}$ ,  $-\text{cation}$ , and  $\text{alkyl}$ .

## Disclosure statement

No potential conflict of interest was reported by the author(s).

## Funding


The authors would like to express their gratitude to Universiti Teknologi Malaysia (UTM) and the Ministry of Higher Education (MOHE) Malaysia for sponsoring this research through the Fundamental Research Grant Scheme (FRGS/1/2019/STG01/UTM/02/7).

## ORCID

Aso Hameed Hasan  <http://orcid.org/0000-0002-8375-1664>

Sonam Shakya  <http://orcid.org/0000-0002-3581-8545>

Sankaranarayanan Murugesan  <http://orcid.org/0000-0002-3680-1577>

Mohammad Rizki Fadhil Pratama  <http://orcid.org/0000-0002-0727-4392>

Joazaizulfazli Jamalis  <http://orcid.org/0000-0002-1756-7244>

## Author contributions

Joazaizulfazli Jamalis, Sankaranarayanan Murugesan and Subhash Chander-supervision, investigation and critical review; Basundhara Das, Subhrajit Biswas, Sonam Shakya and Mohammad Rizki Fadhil Pratama-methodology, software's, investigation, formal analysis, data curation, interpretation of data and revision; Faiq H.S. Hussain, Shajarahtunnur Jamil and Aso Hameed Hasan, design of study, methodology, investigation, and original draft. All authors critically reviewed and approved the manuscript before submission.

## References

- Allen, M. P., & Tildesley, D. J. (2017). *Computer simulation of liquids*. Oxford University Press.
- Anand, P., Singh, B., & Singh, N. (2012). A review on coumarins as acetylcholinesterase inhibitors for Alzheimer's disease. *Bioorganic & Medicinal Chemistry*, 20(3), 1175–1180. <https://doi.org/10.1016/j.bmc.2011.12.042>
- Banerjee, P., Eckert, A. O., Schrey, A. K., & Preissner, R. (2018). ProTox-II: A webserver for the prediction of toxicity of chemicals. *Nucleic Acids Research*, 46(W1), W257–W263. <https://doi.org/10.1093/nar/gky318>
- Baruah, P., Basumatary, G., Yesylevskyy, S. O., Aguan, K., Bez, G., & Mitra, S. (2019). Novel coumarin derivatives as potent acetylcholinesterase inhibitors: Insight into efficacy, mode and site of inhibition. *Journal of Biomolecular Structure & Dynamics*, 37(7), 1750–1765. <https://doi.org/10.1080/07391102.2018.1465853>
- Bolognesi, M. L., Cavalli, A., Valgimigli, L., Bartolini, M., Rosini, M., Andrisano, V., Recanatini, M., & Melchiorre, C. (2007). Multi-target-directed drug design strategy: From a dual binding site acetylcholinesterase inhibitor to a trifunctional compound against Alzheimer's disease. *Journal of Medicinal Chemistry*, 50(26), 6446–6449. <https://doi.org/10.1021/jm701225u>
- Brown, R. C., Lockwood, A. H., & Sonawane, B. R. (2005). Neurodegenerative diseases: An overview of environmental risk factors. *Environmental Health Perspectives*, 113(9), 1250–1256. <https://doi.org/10.1289/ehp.7567>
- Cardoso, S. H., Barreto, M. B., Lourenço, M. C., Henriques, M., Candéa, A. L., Kaiser, C. R., & de Souza, M. V. (2011). Antitubercular activity of new coumarins. *Chemical Biology & Drug Design*, 77(6), 489–493. <https://doi.org/10.1111/j.1747-0285.2011.01120.x>
- Chander, S., Ashok, P., Zheng, Y.-T., Wang, P., Raja, K. S., Taneja, A., & Murugesan, S. (2016). Design, synthesis and in-vitro evaluation of novel tetrahydroquinoline carbamates as HIV-1 RT inhibitor and their antifungal activity. *Bioorganic Chemistry*, 64, 66–73. <https://doi.org/10.1016/j.bioorg.2015.12.005>
- Cheung, J., Rudolph, M. J., Burshteyn, F., Cassidy, M. S., Gary, E. N., Love, J., Franklin, M. C., & Height, J. J. (2012). Structures of human acetylcholinesterase in complex with pharmacologically important ligands. *Journal of Medicinal Chemistry*, 55(22), 10282–10286. <https://doi.org/10.1021/jm300871x>
- Cimler, R., Maresova, P., Kuhnova, J., & Kuca, K. (2019). Predictions of Alzheimer's disease treatment and care costs in European countries. *PLoS One*, 14(1), e0210958. <https://doi.org/10.1371/journal.pone.0210958>
- DeLano, W. L., & Bromberg, S. (2004). *PyMOL user's guide*. DeLano Scientific LLC, 629p.
- Elkollu, M., Chafai, N., Chafaa, S., Kadi, I., Bensouici, C., & Hellal, A. (2022). New phosphinic and phosphonic acids: Synthesis, antidiabetic, anti-Alzheimer, antioxidant activity, DFT study and SARS-CoV-2 inhibition. *Journal of Molecular Structure*, 1268(2022), 133701. <https://doi.org/10.1016/j.molstruc.2022.133701>
- Ellman, G. L., Courtney, K. D., Andres, V., & Feather-Stone, R. M. (1961). A new and rapid colorimetric determination of acetylcholinesterase activity. *Biochemical Pharmacology*, 7(2), 88–95. [https://doi.org/10.1016/0006-2952\(61\)90145-9](https://doi.org/10.1016/0006-2952(61)90145-9)
- Essmann, U., Perera, L., Berkowitz, M. L., Darden, T., Lee, H., & Pedersen, L. G. (1995). A smooth particle mesh Ewald method. *The Journal of Chemical Physics*, 103(19), 8577–8593. <https://doi.org/10.1063/1.470117>
- Fallarero, A., Oinonen, P., Gupta, S., Blom, P., Galkin, A., Mohan, C. G., & Vuorela, P. M. (2008). Inhibition of acetylcholinesterase by coumarins:

- The case of coumarin 106. *Pharmacological Research*, 58(3-4), 215–221. <https://doi.org/10.1016/j.phrs.2008.08.001>
- Fujikawa, F., Hirai, K., Hirayama, T., Nanaumi, A., Umamoto, T., Kawamura, M., Nagami, K. A. Y. A., Nakasone, K., Kaji, M., Kuroiwa, T., Naito, M., Tsukuma, S., & Mabuchi, N. (1969). Studies on chemotherapeutics for Mycobacterium tuberculosis. XXIV. Synthesis and antibacterial activity of Mycobacterium tuberculosis of 3-methoxy-2-phenoxybenzaldehyde, 3-methoxy-4-(3-methoxyphenoxy) benzaldehyde and 3-methoxy-4-(4-methoxyphenoxy) benzaldehyde derivatives. *Yakugaku Zasshi*, 89(9), 1266–1271. [https://doi.org/10.1248/yakushi1947.89.9\\_1266](https://doi.org/10.1248/yakushi1947.89.9_1266)
- Gomha, S. M., Abdel-Aziz, H. M., & El-Reedy, A. A. M. (2018). Facile synthesis of Pyrazolo[3,4-c]pyrazoles bearing coumarine ring as anticancer agents. *Journal of Heterocyclic Chemistry*, 55(8), 1960–1965. <https://doi.org/10.1002/jhet.3235>
- Goyal, D., Kaur, A., & Goyal, B. (2018). Benzofuran and indole: Promising scaffolds for drug development in Alzheimer's disease. *ChemMedChem*, 13(13), 1275–1299. <https://doi.org/10.1002/cmdc.201800156>
- Hadjipavlou-Litina, D., Litinas, K., & Kontogiorgis, C. (2007). The anti-inflammatory effect of coumarin and its derivatives. *Anti-Inflammatory & anti-Allergy Agents in Medicinal Chemistry*, 6(4), 293–306. <https://doi.org/10.2174/187152307783219989>
- Hanwell, M. D., Curtis, D. E., Lonie, D. C., Vandermeersch, T., Zurek, E., & Hutchison, G. R. (2012). Avogadro: An advanced semantic chemical editor, visualization, and analysis platform. *Journal of Cheminformatics*, 4(1), 17. <https://doi.org/10.1186/1758-2946-4-17>
- Hardy, J., & Selkoe, D. J. (2002). The amyloid hypothesis of Alzheimer's disease: Progress and problems on the road to therapeutics. *Science (New York, N.Y.)*, 297(5580), 353–356. <https://doi.org/10.1126/science.1072994>
- Hasan, A. H., Amran, S. I., Hussain, F. H. S., Jaff, B. A., & Jamal, J. (2019). Molecular docking and recent advances in the design and development of cholinesterase inhibitor scaffolds: Coumarin hybrids. *ChemistrySelect*, 4(48), 14140–14156. <https://doi.org/10.1002/slct.201903607>
- Hasan, A. H., Hussain, N. H., Shakya, S., Jamal, J., Pratama, M. R. F., Chander, S., Kharkwal, H., & Murugesan, S. (2022). In silico discovery of multi-targeting inhibitors for the COVID-19 treatment by molecular docking, molecular dynamics simulation studies, and ADMET predictions. *Structural Chemistry*, 33(5), 1645–1665. <https://doi.org/10.1007/s11224-022-01996-y>
- Hasan, A. H., Murugesan, S., Amran, S. I., Chander, S., Alanazi, M. M., Hadda, T. B., Shakya, S., Pratama, M. R. F., Das, B., Biswas, S., & Jamal, J. (2022). Novel thiophene Chalcones-Coumarin as acetylcholinesterase inhibitors: Design, synthesis, biological evaluation, molecular docking, ADMET prediction and molecular dynamics simulation. *Bioorganic Chemistry*, 119, 105572. <https://doi.org/10.1016/j.bioorg.2021.105572>
- Hoerr, R., & Noeldner, M. (2002). Ensaculin (KA-672. HCl): A multitransmitter approach to dementia treatment. *CNS Drug Reviews*, 8(2), 143–158. <https://doi.org/10.1111/j.1527-3458.2002.tb00220.x>
- Hu, Y., Shen, Y., Wu, X., Tu, X., & Wang, G.-X. (2018). Synthesis and biological evaluation of coumarin derivatives containing imidazole skeleton as potential antibacterial agents. *European Journal of Medicinal Chemistry*, 143, 958–969. <https://doi.org/10.1016/j.ejmech.2017.11.100>
- Huang, X. Y., Shan, Z. J., Zhai, H. L., Su, L., & Zhang, X. Y. (2011). Study on the anticancer activity of coumarin derivatives by molecular modeling. *Chemical Biology & Drug Design*, 78(4), 651–658. <https://doi.org/10.1111/j.1747-0285.2011.01195.x>
- Huang, L., Yuan, X., Yu, D., Lee, K., & Chen, C. H. (2005). Mechanism of action and resistant profile of anti-HIV-1 coumarin derivatives. *Virology*, 332(2), 623–628. <https://doi.org/10.1016/j.virol.2004.11.033>
- Humphrey, W., Dalke, A., & Schulten, K. (1996). VMD: Visual molecular dynamics. *Journal of Molecular Graphics*, 14(1), 33–38. [https://doi.org/10.1016/0263-7855\(96\)00018-5](https://doi.org/10.1016/0263-7855(96)00018-5)
- Hussen, N. H., Hasan, A. H., Jamal, J., Shakya, S., Chander, S., Kharkwal, H., Murugesan, S., Ajit Bastikar, V., & Pyarelal Gupta, P. (2022). Potential inhibitory activity of phytoconstituents against black fungus: In silico ADMET, molecular docking and MD simulation studies. *Computational Toxicology (Amsterdam, Netherlands)*, 24, 100247. <https://doi.org/10.1016/j.comtox.2022.100247>
- Hwu, J. R., Singha, R., Hong, S. C., Chang, Y. H., Das, A. R., Vliegen, I., Clercq, E. D., & Neyts, J. (2008). Synthesis of new benzimidazole-coumarin conjugates as anti-hepatitis C virus agents. *Antiviral Research*, 77(2), 157–162. <https://doi.org/10.1016/j.antiviral.2007.09.003>
- Ibrar, A., Zaib, S., Jabeen, F., Iqbal, J., & Saeed, A. (2016). Unraveling the alkaline phosphatase inhibition, anticancer, and antileishmanial potential of coumarin-triazolothiadiazine hybrids: Design, synthesis, and molecular docking analysis. *Archiv Der Pharmazie*, 349(7), 553–565. <https://doi.org/10.1002/ardp.201500392>
- Ibrar, A., Zaib, S., Khan, I., Jabeen, F., Iqbal, J., & Saeed, A. (2015). Facile and expedient access to bis-coumarin-iminothiazole hybrids by molecular hybridization approach: Synthesis, molecular modelling and assessment of alkaline phosphatase inhibition, anticancer and antileishmanial potential. *RSC Advances*, 5(109), 89919–89931. <https://doi.org/10.1039/C5RA14900B>
- Islam, M. M., Rohman, M. A., Gurung, A. B., Bhattacharjee, A., Aguan, K., & Mitra, S. (2018). Correlation of cholinergic drug induced quenching of acetylcholinesterase bound thioflavin-T fluorescence with their inhibition activity. *Spectrochimica Acta. Part A, Molecular and Biomolecular Spectroscopy*, 189, 250–257. <https://doi.org/10.1016/j.saa.2017.08.009>
- Jacquot, Y., Laios, I., Cleeren, A., Nonclercq, D., Bermont, L., Refouvet, B., Boubekeur, K., Xicluna, A., Leclercq, G., & Laurent, G. (2007). Synthesis, structure, and estrogenic activity of 4-amino-3-(2-methylbenzyl)coumarins on human breast carcinoma cells. *Bioorganic & Medicinal Chemistry*, 15(6), 2269–2282. <https://doi.org/10.1016/j.bmc.2007.01.025>
- Jorgensen, W. L., Chandrasekhar, J., Madura, J. D., Impey, R. W., & Klein, M. L. (1983). Comparison of simple potential functions for simulating liquid water. *The Journal of Chemical Physics*, 79(2), 926–935. <https://doi.org/10.1063/1.445869>
- Kalepu, S., & Nekkanti, V. (2015). Insoluble drug delivery strategies: Review of recent advances and business prospects. *Acta Pharmaceutica Sinica. B*, 5(5), 442–453. <https://doi.org/10.1016/j.apsb.2015.07.003>
- Katalinić, M., Rusak, G., Domaćinović Barović, J., Šinko, G., Jelić, D., Antolović, R., & Kovarić, Z. (2010). Structural aspects of flavonoids as inhibitors of human butyrylcholinesterase. *European Journal of Medicinal Chemistry*, 45(1), 186–192. <https://doi.org/10.1016/j.ejmech.2009.09.041>
- Kawsar, S., Hosen, M. A., Chowdhury, T. S., Rana, K. M., Fujii, Y., & Ozeki, Y. (2021). Thermochemical, PASS, molecular docking, drug-likeness and in silico ADMET prediction of cytidine derivatives against HIV-1 reverse transcriptase. *Revista de Chimie*, 72(3), 159–178. <https://doi.org/10.37358/RC.21.3.8446>
- Khan, M. D., Shakya, S., Vu, H. H. T., Habte, L., & Ahn, J. W. (2021). Low concentrated phosphorus sorption in aqueous medium on aragonite synthesized by carbonation of seashells: Optimization, kinetics, and mechanism study. *Journal of Environmental Management*, 280, 111652. <https://doi.org/10.1016/j.jenvman.2020.111652>
- Khodair, A. I., Alsafi, M. A., & Nafie, M. S. (2019). Synthesis, molecular modeling and anti-cancer evaluation of a series of quinazoline derivatives. *Carbohydrate Research*, 486(2019), 107832. <https://doi.org/10.1016/j.carres.2019.107832>
- Kontogiorgis, C., Detsi, A., & Hadjipavlou-Litina, D. (2012). Coumarin-based drugs: A patent review (2008 – present). *Expert Opinion on Therapeutic Patents*, 22(4), 437–454. <https://doi.org/10.1517/13543776.2012.678835>
- Kostova, I., Bhatia, S., Grigorov, P., Balkansky, S., Parmar, V. S., Prasad, A. K., & Saso, L. (2011). Coumarins as antioxidants. *Current Medicinal Chemistry*, 18(25), 3929–3951. <https://doi.org/10.2174/092986711803414395>
- Kufareva, I., & Abagyan, R. (2012). Methods of protein structure comparison. *Methods in Molecular Biology (Clifton, N.J.)*, 857, 231–257. [https://doi.org/10.1007/978-1-61779-588-6\\_10](https://doi.org/10.1007/978-1-61779-588-6_10)
- Kumar, R., Saha, A., & Saha, D. (2012). A new antifungal coumarin from *Clausena excavata*. *Fitoterapia*, 83(1), 230–233. <https://doi.org/10.1016/j.fitote.2011.11.003>
- Lee, S. K., Achieng, E., Maddox, C., Chen, S. C., Iuvone, P. M., & Fukuhara, C. (2011). Extracellular low pH affects circadian rhythm expression in human primary fibroblasts. *Biochemical and Biophysical Research Communications*, 416(3-4), 337–342. <https://doi.org/10.1016/j.bbrc.2011.11.037>
- Leonetti, F., Favia, A., Rao, A., Aliano, R., Paluszczak, A., Hartmann, R. W., & Carotti, A. (2004). Design, synthesis, and 3D QSAR of novel potent and selective aromatase inhibitors. *Journal of Medicinal Chemistry*, 47(27), 6792–6803. <https://doi.org/10.1021/jm049535j>

- Liu, H.-r., Liu, X.-j., Fan, H.-q., Tang, J.-j., Gao, X.-h., & Liu, W.-K. (2014). Design, synthesis and pharmacological evaluation of chalcone derivatives as acetylcholinesterase inhibitors. *Bioorganic & Medicinal Chemistry*, 22(21), 6124–6133. <https://doi.org/10.1016/j.bmc.2014.08.033>
- Liu, H., Liu, L., Gao, X., Liu, Y., Xu, W., He, W., Jiang, H., Tang, J., Fan, H., & Xia, X. (2017). Novel ferulic amide derivatives with tertiary amine side chain as acetylcholinesterase and butyrylcholinesterase inhibitors: The influence of carbon spacer length, alkylamine and aromatic group. *European Journal of Medicinal Chemistry*, 126, 810–822. <https://doi.org/10.1016/j.ejmech.2016.12.003>
- Luscombe, N. M., Laskowski, R. A., & Thornton, J. M. (2001). Amino acid–base interactions: A three-dimensional analysis of protein–DNA interactions at an atomic level. *Nucleic Acids Research*, 29(13), 2860–2874. <https://doi.org/10.1093/nar/29.13.2860>
- Marzouk, A. A., Abdel-Aziz, S. A., Abdelrahman, K. S., Wanas, A. S., Gouda, A. M., Youssif, B. G. M., & Abdel-Aziz, M. (2020). Design and synthesis of new 1,6-dihydropyrimidin-2-thio derivatives targeting VEGFR-2: Molecular docking and antiproliferative evaluation. *Bioorganic Chemistry*, 102(2020), 104090. <https://doi.org/10.1016/j.bioorg.2020.104090>
- Mathew, B., Mathew, G. E., Uçar, G., Baysal, I., Suresh, J., Mathew, S., Haridas, A., & Jayaprakash, V. (2016). Potent and selective monoamine oxidase-B inhibitory activity: Fluoro-vs. trifluoromethyl-4-hydroxylated chalcone derivatives. *Chemistry & Biodiversity*, 13(8), 1046–1052. <https://doi.org/10.1002/cbdv.201500367>
- McKhann, G. M., Knopman, D. S., Chertkow, H., Hyman, B. T., Jack, C. R., Kawas, C. H., Klunk, W. E., Koroshetz, W. J., Manly, J. J., Mayeux, R., Mohs, R. C., Morris, J. C., Rossor, M. N., Scheltens, P., Carrillo, M. C., Thies, B., Weintraub, S., & Phelps, C. H. (2011). The diagnosis of dementia due to Alzheimer's disease: Recommendations from the National Institute on Aging–Alzheimer's Association workgroups on diagnostic guidelines for Alzheimer's disease. *Alzheimer's & Dementia: The Journal of the Alzheimer's Association*, 7(3), 263–269. <https://doi.org/10.1016/j.jalz.2011.03.005>
- Melagraki, G., Afantitis, A., Igglessi-Markopoulou, O., Detsi, A., Koufaki, M., Kontogiorgis, C., & Hadjipavlou-Litina, D. J. (2009). Synthesis and evaluation of the antioxidant and anti-inflammatory activity of novel coumarin-3-aminoamides and their alpha-lipoic acid adducts. *European Journal of Medicinal Chemistry*, 44(7), 3020–3026. <https://doi.org/10.1016/j.ejmech.2008.12.027>
- Minhas, R., Sandhu, S., Bansal, Y., & Bansal, G. (2017). Benzoxazole-coumarin derivatives: Potential candidates for development of safer anti-inflammatory drugs. *Der Chemica Sinica*, 8(1), 146–157. <https://doi.org/10.1016/j.ejmech.2008.12.027>
- Morris, G. M., Goodsell, D. S., Halliday, R. S., Huey, R., Hart, W. E., Belew, R. K., & Olson, A. J. (1998). Automated docking using a Lamarckian genetic algorithm and an empirical binding free energy function. *Journal of Computational Chemistry*, 19(14), 1639–1662. [https://doi.org/10.1002/\(SICI\)1096-987X\(19981115\)19:14 < 1639::AID-JCC10 > 3.0.CO;2-B](https://doi.org/10.1002/(SICI)1096-987X(19981115)19:14 < 1639::AID-JCC10 > 3.0.CO;2-B)
- NA. (2015). 2015 Alzheimer's disease facts and figures. *Alzheimer's & Dementia: The Journal of the Alzheimer's Association*, 11(3), 332–384. <https://doi.org/10.1016/j.jalz.2015.02.003>
- NA. (2019). 2019 Alzheimer's disease facts and figures. *Alzheimer's & Dementia*, 15(3), 321–387. <https://doi.org/10.1016/j.jalz.2019.01.010>
- Nafie, M. S., Tantawy, M. A., & Elmgheed, G. A. (2019). Screening of different drug design tools to predict the mode of action of steroidal derivatives as anti-cancer agents. *Steroids*, 152(2019), 108485. <https://doi.org/10.1016/j.steroids.2019.108485>
- Nam, S. O., Park, D. H., Lee, Y. H., Ryu, J. H., & Lee, Y. S. (2014). Synthesis of aminoalkyl-substituted coumarin derivatives as acetylcholinesterase inhibitors. *Bioorganic & Medicinal Chemistry*, 22(4), 1262–1267. <https://doi.org/10.1016/j.bmc.2014.01.010>
- Nepali, K., Lee, H.-Y., & Liou, J.-P. (2019). Nitro-group-containing drugs. *Journal of Medicinal Chemistry*, 62(6), 2851–2893. <https://doi.org/10.1021/acs.jmedchem.8b00147>
- Patterson, C. (2018). *World Alzheimer report 2018: The state of the art of dementia research: New frontiers*. Alzheimer's Disease International (ADI), pp. 32–36.
- Petersen, E. F., Goddard, T. D., Huang, C. C., Couch, G. S., Greenblatt, D. M., Meng, E. C., & Ferrin, T. E. (2004). UCSF Chimera—A visualization system for exploratory research and analysis. *Journal of Computational Chemistry*, 25(13), 1605–1612. <https://doi.org/10.1002/jcc.20084>
- Picciotto, M. R., Higley, M. J., & Mineur, Y. S. (2012). Acetylcholine as a neuromodulator: Cholinergic signaling shapes nervous system function and behavior. *Neuron*, 76(1), 116–129. <https://doi.org/10.1016/j.neuron.2012.08.036>
- Poli, G., Martinelli, A., & Tuccinardi, T. (2016). Reliability analysis and optimization of the consensus docking approach for the development of virtual screening studies. *Journal of Enzyme Inhibition and Medicinal Chemistry*, 31(sup2), 167–173. <https://doi.org/10.1080/14756366.2016.1193736>
- Prasanna, S., & Doerksen, R. J. (2009). Topological polar surface area: A useful descriptor in 2D-QSAR. *Current Medicinal Chemistry*, 16(1), 21–41. <https://doi.org/10.2174/092986709787002817>
- Salih, R. H. H., Hasan, A. H., Hussein, A. J., Samad, M. K., Shakya, S., Jamalis, J., Hawaiz, F. E., & Pratama, M. R. F. (2022). One-pot synthesis, molecular docking, ADMET, and DFT studies of novel pyrazolines as promising SARS-CoV-2 main protease inhibitors. *Research on Chemical Intermediates*, 48(11), 4729–4751. <https://doi.org/10.1007/s11164-022-04831-5>
- Saeed, A., Zaib, S., Ashraf, S., Iftikhar, J., Muddassar, M., Zhang, K. Y. J., & Iqbal, J. (2015). Synthesis, cholinesterase inhibition and molecular modelling studies of coumarin linked thiourea derivatives. *Bioorganic Chemistry*, 63, 58–63. <https://doi.org/10.1016/j.bioorg.2015.09.009>
- Şahin, Ö., Özmen Özdemir, Ü., Seferoğlu, N., Adem, Ş., & Seferoğlu, Z. (2022). Synthesis, characterization, molecular docking, and in vitro screening of new metal complexes with coumarin Schiff base as anticholine esterase and antipancreatic cholesterol esterase agents. *Journal of Biomolecular Structure & Dynamics*, 40(10), 4460–4474. <https://doi.org/10.1080/07391102.2020.1858163>
- Sameem, B., Saeedi, M., Mahdavi, M., Nadri, H., Moghadam, F. H., Edraki, N., Khan, M. I., & Amini, M. (2017). Synthesis, docking study and neuroprotective effects of some novel pyrano[3,2-c]chromene derivatives bearing morpholine/phenylpiperazine moiety. *Bioorganic & Medicinal Chemistry*, 25(15), 3980–3988. <https://doi.org/10.1016/j.bmc.2017.05.043>
- Saravanan, K., Karthikeyan, S., Sugarthi, S., & Stephen, A. D. (2021). Binding studies of known molecules with acetylcholinesterase and bovine serum albumin: A comparative view. *Spectrochimica Acta. Part A, Molecular and Biomolecular Spectroscopy*, 259, 119856. <https://doi.org/10.1016/j.saa.2021.119856>
- Savjani, K. T., Gajjar, A. K., & Savjani, J. K. (2012). Drug solubility: Importance and enhancement techniques. *ISRN Pharmaceutics*, 2012, 195727. <https://doi.org/10.5402/2012/195727>
- Scarpini, E., Scheltens, P., & Feldman, H. (2003). Treatment of Alzheimer's disease: Current status and new perspectives. *The Lancet. Neurology*, 2(9), 539–547. [https://doi.org/10.1016/S1474-4422\(03\)00502-7](https://doi.org/10.1016/S1474-4422(03)00502-7)
- Sivakumar, M., Saravanan, K., Saravanan, V., Sugarthi, S., Kumar, S. M., Alhaji Isa, M., Rajakumar, P., & Aravindhan, S. (2020). Discovery of new potential triplet acting inhibitor for Alzheimer's disease via X-ray crystallography, molecular docking and molecular dynamics. *Journal of Biomolecular Structure & Dynamics*, 38(7), 1903–1917. <https://doi.org/10.1080/07391102.2019.1620128>
- Tasso, B., Catto, M., Nicolotti, O., Novelli, F., Tonelli, M., Giangreco, I., Pisani, L., Sparatore, A., Boido, V., Carotti, A., & Sparatore, F. (2011). Quinolizidinyl derivatives of bi-and tricyclic systems as potent inhibitors of acetyl- and butyrylcholinesterase with potential in Alzheimer's disease. *European Journal of Medicinal Chemistry*, 46(6), 2170–2184. <https://doi.org/10.1016/j.ejmech.2011.02.071>
- Tran, T.-D., Nguyen, T.-C.-V., Nguyen, N.-S., Nguyen, D.-M., Nguyen, T.-T.-H., Le, M.-T., & Thai, K.-M. (2016). Synthesis of novel chalcones as acetylcholinesterase inhibitors. *Applied Sciences*, 6(7), 198. <https://doi.org/10.3390/app6070198>
- Trott, O., & Olson, A. J. (2010). AutoDock Vina: Improving the speed and accuracy of docking with a new scoring function, efficient optimization, and multithreading. *Journal of Computational Chemistry*, 31(2), 455–461. <https://doi.org/10.1002/jcc.21334>
- Uriarte-Pueyo, I., & Calvo, M. I. (2011). Flavonoids as acetylcholinesterase inhibitors. *Current Medicinal Chemistry*, 18(34), 5289–5302. <https://doi.org/10.2174/092986711798184325>
- Uttarkar, A., Kishore, A. P., Srinivas, S. M., Rangappa, S., Kusanur, R., & Niranjana, V. (2022). Coumarin derivative as a potent drug candidate

- against triple negative breast cancer targeting the frizzled receptor of wingless-related integration site signaling pathway. *Journal of Biomolecular Structure and Dynamics*. <https://doi.org/10.1080/07391102.2021.2022536>
- Vanommeslaeghe, K., Hatcher, E., Acharya, C., Kundu, S., Zhong, S., Shim, J., Darian, E., Guvench, O., Lopes, P., & Vorobyov, I. (2010). CHARMM general force field: A force field for drug-like molecules compatible with the CHARMM all-atom additive biological force fields. *Journal of Computational Chemistry*, 31(4), 671–690. <https://doi.org/10.1002/jcc.21367>
- Vasconcelos, J. F., Teixeira, M. M., Barbosa-Filho, J. M., Agra, M. F., Nunes, X. P., Giulietti, A. M., Ribeiro-dos-Santos, R., & Soares, M. B. (2009). Effects of umbelliferone in a murine model of allergic airway inflammation. *European Journal of Pharmacology*, 609(1-3), 126–131. <https://doi.org/10.1016/j.ejphar.2009.03.027>
- Vilar, S., Chakrabarti, M., & Costanzi, S. (2010). Prediction of passive blood–brain partitioning: Straightforward and effective classification models based on in silico derived physicochemical descriptors. *Journal of Molecular Graphics & Modelling*, 28(8), 899–903. <https://doi.org/10.1016/j.jmglm.2010.03.010>
- Wade, R. C., & Goodford, P. J. (1989). The role of hydrogen-bonds in drug binding. *Progress in Clinical and Biological Research*, 289, 433–444.
- Wang, L., Wang, Y., Tian, Y., Shang, J., Sun, X., Chen, H., Wang, H., & Tan, W. (2017). Design, synthesis, biological evaluation, and molecular modeling studies of chalcone-rivastigmine hybrids as cholinesterase inhibitors. *Bioorganic & Medicinal Chemistry*, 25(1), 360–371. <https://doi.org/10.1016/j.bmc.2016.11.002>
- Wu, S., & Zhang, Y. (2008). A comprehensive assessment of sequence-based and template-based methods for protein contact prediction. *Bioinformatics (Oxford, England)*, 24(7), 924–931. <https://doi.org/10.1093/bioinformatics/btn069>
- Yang, Z., Zhang, D., Ren, J., Yang, M., & Li, S. (2012). Acetylcholinesterase inhibitory activity of the total alkaloid from traditional Chinese herbal medicine for treating Alzheimer's disease. *Medicinal Chemistry Research*, 21(6), 734–738. <https://doi.org/10.1007/s00044-011-9582-8>
- Yu, W., He, X., Vanommeslaeghe, K., & MacKerell, A. D. Jr. (2012). Extension of the CHARMM general force field to sulfonyl-containing compounds and its utility in biomolecular simulations. *Journal of Computational Chemistry*, 33(31), 2451–2468. <https://doi.org/10.1002/jcc.23067>
- Zaout, S., Chafaa, S., Hellal, A., Boukhemis, O., Khattabi, L., Merazig, H., Chafai, N., Bensouici, C., & Bendjeddou, L. (2021). Hydroxyphenylamine phosphonate derivatives: Synthesis, X-ray crystallographic analysis, and evaluation of their anti-Alzheimer effects and antioxidant activities. *Journal of Molecular Structure*, 1225, 129121. <https://doi.org/10.1016/j.molstruc.2020.129121>
- Zhang, Y.-M., Lu, Y.-J., & Rock, C. O. (2004). The reductase steps of the type II fatty acid synthase as antimicrobial targets. *Lipids*, 39(11), 1055–1060. <https://doi.org/10.1007/s11745-004-1330-3>
- Zhang, X., Rakesh, K., Bukhari, S., Balakrishna, M., Manukumar, H., & Qin, H.-L. (2018). Multi-targetable chalcone analogs to treat deadly Alzheimer's disease: Current view and upcoming advice. *Bioorganic Chemistry*, 80(2018), 86–93. <https://doi.org/10.1016/j.bioorg.2018.06.009>